Spacer Design for Membrane Distillation Module Using CFD

Author

Ali Aitzaz

Registration Number

00000104468

Thesis Supervisor

Dr. Zaib Ali

DEPARTMENT OF MECHANICAL ENGINEERING

SCHOOL OF MECHANICAL & MANUFACTURING ENGINEERING

NATIONAL UNIVERSITY OF SCIENCES AND TECHNOLOGY

ISLAMABAD

SEPTEMBER 2020

Spacer Design for Membrane Distillation Module Using CFD

Author

Ali Aitzaz

Registration Number

00000104468

A thesis submitted in partial fulfillment of the requirements for the degree of

MS Mechanical Engineering

Thesis Supervisor:

Dr. Zaib Ali

Thesis Supervisor's Signature:

_____

DEPARTMENT OF MECHANICAL ENGINEERING

SCHOOL OF MECHANICAL & MANUFACTURING ENGINEERING

NATIONAL UNIVERSITY OF SCIENCES AND TECHNOLOGY

ISLAMABAD

SEPTEMBER 2020

Declaration

I certify that this research work titled "*Spacer Design for Membrane Distillation Module Using CFD"* is my own work. The work has not been presented elsewhere for assessment. The material that has been used from other sources it has been properly acknowledged / referred.

Signature of Student

Ali Aitzaz

00000104468

Plagiarism Certificate (Turnitin Report)

This thesis has been checked for Plagiarism. Turnitin report endorsed by Supervisor is attached.

Signature of Student

Ali Aitzaz

Registration Number

00000104468

Signature of Supervisor

Copyright Statement

Acknowledgments

There is indeed nothing that can be done in this world without the consent of Almighty Allah so I would start by thanking Him who has bestowed enough mental and physical capability that I could take this challenge on and accomplish this feat of extreme honor. All praises and thanks to Him who has constantly showered His blessings in various forms to help me reach this point.

The role of parents and family can never be undermined so they are absolute firsts from this world's physical beings. Since bringing me and my siblings in this world, my parents have always supported us and tried to provide everything possible to mold me and my siblings to our best shape. Along with parents, siblings have always been there even when parents got strict or could not understand, they understood and have been a constant support system.

For this academic achievement, I would like to start by expressing my gratitude to my supervisor Dr. Zaib Ali for his guidance, consistent support, and compassion throughout my tenure here being a master's student.

Next in line are my friends and fellows both in class and otherwise. They have pushed and motivated me in all possible ways to complete my degree and get on with life. A special shoutout to Zia and Asfand for their constant guidance throughout, no matter the time I called, they guided and assisted me wherever required. Another special person to be mentioned here is Owais aka Ejaz Saab for being the partner in crime and burning the midnight oil together, especially towards the end of our degree. We have made some good memories along the way that will be cherished.

I would also like to thank Dr. Emad Uddin, Dr. Muhammad Sajid, and Dr. Samiur Rehman Shah for being on my thesis guidance and evaluation committee.

And with that, I conclude by expressing my gratitude to all the individuals who have been the torchbearers for my study.

Dedicated to my exceptional parents and adored siblings whose tremendous support and cooperation led me to this wonderful accomplishment.

Abstract

Membrane processes are used widely to desalinate water. Major techniques for this purpose include Reverse Osmosis (RO), Multi-stage Flash Distillation (MSD), Membrane Distillation (MD) and Multi-effect Distillation (MED) with RO being most used. Higher salt rejection rate of MD (99%) than that of RO (96%) makes it a better option for water desalination. Direct Contact Membrane Distillation (DCMD) is the easiest configuration among others for MD at low temperature and pressure conditions thus reducing cost.

CFD study of impact of spacer in feed and permeate channels has been conducted by considering the effect of velocity, membrane thickness, spacer filament distance and their arrangement variants. Temperature Polarization Index (TPI) and Vapor Flux are used as the evaluation criteria for performance of a combination. Study shows that TPI is lower and thus performance of DCMD setup is better for a combination of high feed and permeate velocity, larger filament diameter arranged mid channel using a thicker membrane in a counter flow arrangement. This can be used to design an effective hybrid desalination system to attain maximum flux.

Table of Content

List of Figures

List of Tables

Chapter 1: Introduction

Water is an essential requirement of life on Earth. It is important not only for humans but for all living beings alike. Applications of water in daily life as well as in industry are countless and with increasing population and industrialization in the world, demand of clean water has increased many folds. Clean water includes not only drinkable water but water that can be used in daily chores and industry.

1.1 Water Content on Earth

Earth contains water on 71% of its surface while all humans and other land dwellers make up the rest 29% of earth's surface with continents and islands. Out of this 71%, only 3.5% is fresh water that can be used by humans. This 3.5% includes lakes and frozen water sources i.e. glaciers and polar ice caps. 69% of fresh water on Earth is in its frozen form. [01]

The water makes up a thin layer on the surface of earth. If we combine all the water on earth and put it at one place, it will measure to 1,386 million km^3 in volume and will cover a small portion of the total volume of globe as represented in fig-1 below.

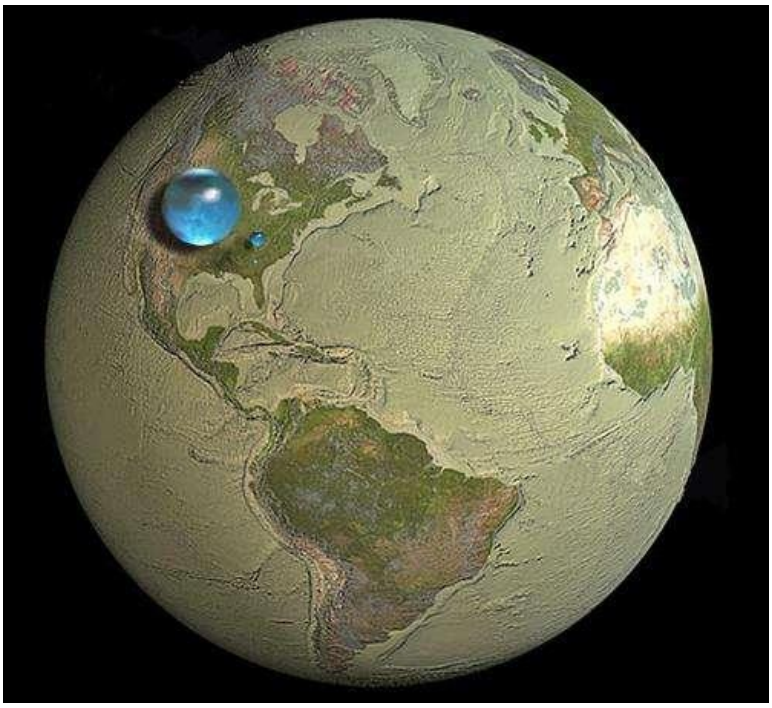

Figure 1. Illustration showing all of Earth's water [02]

The largest sphere represents all the water of earth including everything from oceans to human body's water content. The smaller sphere on the right represents the fresh water including rivers, lakes, and groundwater. Right below that sphere is a tiny sphere that represents fresh water accessible to humans and other living beings [02]. This figure truly helps realizing the limited quantity of fresh water we have at our disposal.

1.2 Water Crisis in Pakistan

Water scarcity is a major challenge for many countries in coming years. World Resources Institute have categorized 164 countries of the world into levels according to their baseline water stress [03]. Pakistan is among the 17 countries at the worst level, extremely high. List of extremely high and high baseline water stress countries is presented in fig-2. The major reasons include the growing population and thus their demand coupled with lack of proper storage and conservation mechanism for water in the country. International Monetary Fund (IMF) in their report on Water Challenges [04] ranked Pakistan at third place in 2015 for countries to undergo extreme water shortage. On the same lines, Pakistan Council of Research in Water Resources (PCRWR) alarmed the authorities about the water shortage and stated that there may be very limited or no clean water in Pakistan by 2025 [05].

Figure 2. Water Stress Rankings by country [03]

With water being a major issue of the world, there have been many efforts to investigate the possibilities of utilizing water available in oceans that is normally not used due to high concentration of salts. Similarly, the ways of reusing and recycling water for agricultural or industrial applications has been under investigation for a few decades. Processes like Reverse Osmosis and Ultrafiltration are being used to treat water in industrial, medical, and other applications including water purification system at homes.

1.3 Water Treatment

Membrane Distillation is a very promising aspect in water treatment. The process surfaced in 1960s [06] and is still under investigation for industrial application owing to its limitation of membrane and its longevity. Reverse Osmosis (RO) is a pressure driven membrane distillation process and amounts up to half of world's water distillation capacity [07]. There are two major reasons RO is not used in Pakistan. Firstly, due to high salinity of the major water source at our disposal, Arabian Sea, causing fouling in membranes for RO. Operating cost to overcome this by changing membranes repeatedly is not feasible. Secondly, there are harmful algae blooms (HABs) in the sea. They contain toxins that can pass through the RO membranes thus reaching reservoirs of drinking water. This may lead to severe consequences leading up to death [08]. Next best option for water desalination is Membrane Distillation.

Water treatment plants installed near water reservoirs are utilized mainly for wastewater treatment in Pakistan. Other than those, mineral water factories have their own filtration plants where fresh water from rivers and lakes is processed to obtain required mineral content. There are various smaller scale water filtration plants installed for human consumption in major cities of Pakistan, working on the principle of RO. Major financial challenge for these plants is the cost of energy and filter replacement. MD process can reduce the energy consumption by many folds being a temperature difference-based process. The required energy for heating the feed solution can be reduced by incorporating solar energy.

1.4 Scope of Work

Recent developments in MD are focused on improvements in geometry of desalination setup and towards understanding the factors affecting permeate flux and membrane integrity to maximize the obtained flux. Owing to its flexibility towards energy source and simplicity of design, DCMD has been a major focus of research in recent past. Inclusion of spacer

technology in feed and permeate channel to reduce Temperature Polarization Index (TPI) and increase turbulence resulting in increased mass flux is a recent development. This study also focuses on the spacer technology in combination with different operational parameters of MD to investigate the optimum operating conditions for maximum mass flux.

Chapter 2: Literature Review

Desalination techniques are utilized in various region of world to meet the demand of clean water [09 – 12]. A major advantage of temperature driven membrane distillation techniques over other pressure driven processes like RO is less sensitivity of its performance on feed concentration. Another bright point for membrane distillation is that its operating temperature and pressures are lower, and the membranes used are more resistant to faults like fouling [13 – 15].

2.1 Membrane Distillation

Membrane Distillation (MD) is a membrane separation process whose driving force is temperature difference across the membrane [13]. A porous hydrophobic membrane is used in (MD) for water treatment that does not allow water molecules to pass through, but vapors can flow through it. The reason behind this selective permeability is pore size of membrane that is lower than diameter of a water molecule. A hot stream of saline water termed as feed is flown on one side of membrane. The high temperature causes vaporization, and they seem through the membrane to other side. A cold fluid is flown on the other side of membrane termed as permeate solution [15]. For water distillation, permeate solution it normally water. It collects and condenses the water vapors coming through the membrane thus adding to the net volume of clean water.

There are four basic configurations of Membrane Distillation pertaining to the method of creating the required pressure difference on both sides of membrane i.e. Direct Contact Membrane Distillation (DCMD), Vacuum Membrane Distillation (VMD), Sweep Gas Membrane Distillation (SGMD) and Air Gap Membrane Distillation (AGMD), each with their own advantages and disadvantages [16 – 18]. They are all briefly explained below with a pictorial summary given in fig-3.

2.1.1 Direct Contact Membrane Distillation (DCMD)

This is the simplest configuration where hot feed water and cold permeate water are both in contact with the hydrophobic membrane on either side, fig-2A. It produces a stable permeate flux and has higher output ratio than other modes. It is the best suited configuration to remove volatiles form the feed solution [15].

At the same time, DCMD has highest thermal polarization and the resultant flux is highly dependent on the concentration of feed solution. It produces relatively lower flux than VMD and the flux quality is very sensitive to pore wetting phenomenon.

2.1.2 Air Gap Membrane Distillation (AGMD)

Air is used on permeate side to create the required pressure difference in this configuration, fig-2B. IT produces lowest thermal losses among other configurations. Pore wetting risk is taken out on permeate side and membrane fouling is also minimized [18].

The additional layer of air gap creates additional resistance in mass transfer and has lowest output ratio. Module design as well as numerical modelling is difficult owing to multiple variables [14].

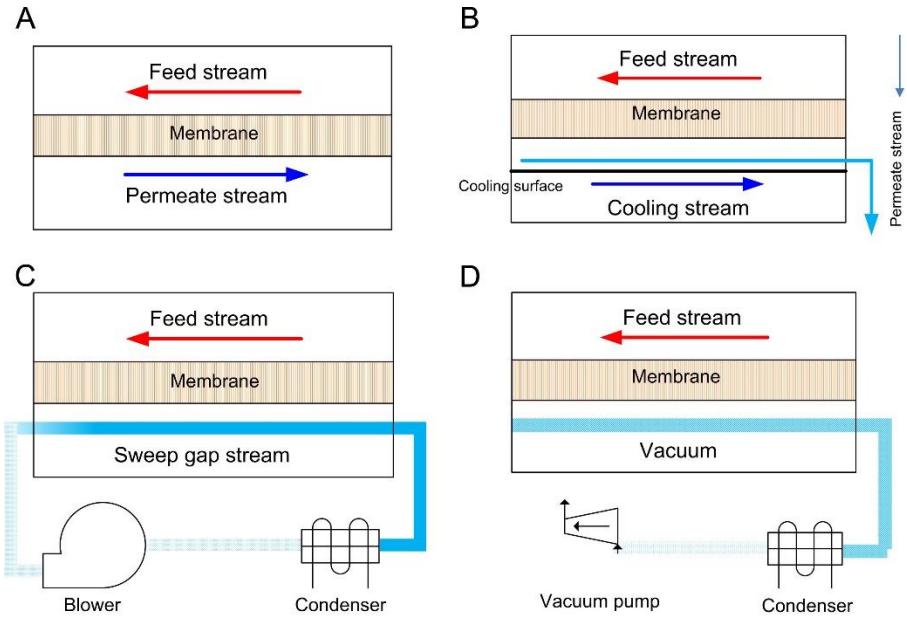

Figure 3. MD Configurations: A) DCMD, B) AGMD, C) SGMD, D) VMD [18]

2.1.3 Sweep Gas Membrane Distillation (SGMD)

Instead of Air, an inert gas is usually used to collect the vapours on permeate side, fig-2C. It produces a high permeate flux and has lower thermal polarization. Pore wetting on permeate side is minimized due to sweep gas and can remove volatiles and aroma compounds.

Heat recovery in SGMD is a difficult task and has additional complexity in design. Distillate flux is on the lower side and gas stream needs to be cleaned and dried [16].

2.1.4 Vacuum Membrane Distillation (VMD)

A vacuum is created on the permeate side to maintain the pressure difference on permeate side, fig-2D. It has lowest thermal polarization among MD configurations. Pore wetting is not a factor due to absence of liquid on permeate side of membrane. It has better scope for concentrating purposes of aqueous streams.

It requires an external condenser and vacuum pump for operation, can be subject to higher fouling and has lower range for volatiles [18].

2.2 Factors Affecting MD Output Flux

Ever since the introduction of MD in 1960s, there have been many efforts to study the effect of operating conditions on the process. Sulaiman et al. [19] reported that feed temperature and feed flow rate impacted the mass flux directly while the concentration of feed solution inversely affected the flux. Membrane selection is also an important aspect of MD process. Membrane thickness and its porosity play important role in determining the mass flux produced. Increasing the porosity of membrane can increase flux by providing more surface area for vapours to pass through. On the other hand, increasing membrane thickness produces more resistance to mass transfer thus reducing the produced flux [20]. In addition to that, thermal and chemical stability, low fouling, and high Liquid Entry Pressure (LEP) for water is desired for a hydrophobic membrane [17].

2.3 Temperature Polarization

Temperature Polarization (TP) is an important factor to consider in MD. Inlet temperature of feed or permeate solution is not the same at the membrane surface that causes a reduced flux. It is measured as Temperature Polarization Index (TPI). It is defined as the ratio of temperature difference of inlet feed and permeate streams and the difference of temperatures on the membrane walls [20]. Mathematically,

$$TPI = \frac{T_f - T_p}{T_{mf} - T_{mp}} \qquad Eq.\ 1$$

Where T_f and T_p are the inlet temperatures of feed and permeate channels. T_{mf} and T_{mp} are the temperatures at membrane surface on feed and permeate side, respectively. Higher the

TPI, lesser is the permeate produced [17]. So, it is desirable to have a smaller value of TPI to attain maximum flux.

2.4 Spacers in DCMD

Temperature polarization is accompanied by Concentration Polarization (CP) as well. CP is the result of salt deposit on membrane pores with time during desalination. Martinez et al. [21 – 23] studied the effect of spacers and stated that spacers' introduction creates turbulence in feed channel which in turn decreases TP. He et al. [24] also compared the effect of TP and CP on permeate flux reduction using brine feed solution. Effect of TP was the prominent one in reducing flux for MD Process.

Impact of module geometry for DCMD was reviewed by Martinez et al. [23] where they compared the flux generated through varying membrane and module design including spacers. Hollow cylindrical arrangement of DCMD module produced better results than flat plat owing to its greater contact surface. Similar results were reported by Chang et al [30].

Effect of spacers on vapor flux by reducing CP and TP has been studied by many researchers [25 – 41] to enhance DCMD performance. Major contributor in reducing CP and TP is mixing and changing the flow pattern of solution due to spacers [34, 40, 42, 43]. Effect of spacers on heat transfer through spacer filled channels was studied by Shakaib et al [31] who reported enhanced heat transfer through the feed and permeate channels. Cipollina et al [33] analysed the module geometry and resulting mass flux for DCMD and the results agreed of the above mentioned. Increased mass flux was noted for spacer filled channels due to increased turbulence.

Spiral wound module for MD has also been studied for impact of spacers by Song et al [36] who reported increased flow mixing in spacer filled channels. In addition to MD, effect of spacers in RO and nanofiltration processes has also been studied [37,38]. Introduction of spacer channels in their studies has been reported to enhance flow mixing and fluctuating flow pattern. This fluctuation has increased the mass flux for RO and nanofiltration.

A combination of spacer arrangement in feed and permeate channels, filament size and their inter-filament distance is investigated in this project. Effect of velocity and membrane thickness at a specific inlet velocity of feed and permeate streams is incorporated to find an optimum arrangement and operating conditions.

Chapter 3: Methodology

Mathematical and computational models are used in this project to evaluate performance of DCMD setup for desalination.

3.1 Mathematical Model

Membrane distillation is a temperature driven process where temperature difference across the membrane surfaces creates pressure gradient resulting in transport of permeate in the form of water vapors. Heat transfer takes place at three different regions, so it can be divided into feed, membrane and permeates sides [20]. In feed and permeate sides, heat is transferred through convection to the environment through convection and as a result of fluid motion through the channels. For membrane, heat is transferred through conduction due to temperature gradient as well as through vapor transport. We can summarize it as:

Feed Side Heat Transfer

$$Q_f = Q_{f,conv} + Q_{f,mol} = h_f\left(T_f - T_{mf}\right) + J_w H_{L,f}\left\{\frac{T_f + T_{mf}}{2}\right\} \qquad Eq.\ 2$$

Permeate Side Heat Transfer

$$Q_p = Q_{p,conv} + Q_{p,mol} = h_p\left(T_{mp} - T_p\right) + J_w H_{L,p}\left\{\frac{T_p + T_{mp}}{2}\right\} \qquad Eq.\ 3$$

Membrane Heat Transfer

$$Q_m = Q_{m,cond} + Q_{m,mol} = h_m\left(T_{mf} - T_{mp}\right) + J_w H_v \qquad Eq.\ 4$$

Literature suggests that in feed and permeate sides, convection is the dominant heat transfer mechanism and effect of molecular heat transfer is negligible. Whereas, through the membrane, both modes of heat transfer amount to be considerable. Equations 2 – 4 can be simplified as:

$$Q_f = h_f\left(T_f - T_{mf}\right) \qquad Eq.\ 5$$

$$Q_p = h_p(T_{mp} - T_p) \quad \text{Eq. 6}$$

$$Q_m = h_m(T_{mf} - T_{mp}) + J_w \Delta H_v \quad \text{Eq. 7}$$

Heat transfer coefficients for both feed and permeate channels can be determined using Nusslet Number (Nu) which in turn can be calculated using Reynolds Number (Re) and Prandtl Number (Pr) for the said flow.

$$h = \frac{Nuk}{d} \quad \text{Eq. 8}$$

Flow conditions in this study reflect to a Reynold's number in laminar flow range and for these conditions, Nu is calculated using:

$$Nu = 1.86\left(\frac{RePrd}{l}\right)^{0.33} \quad \text{Eq. 9}$$

Whereas, Re and Pr can be calculated using the following relations.

$$Re = \frac{\rho v d}{\mu} \quad \text{Eq. 10}$$

$$Pr = \frac{\mu C_p}{k} \quad \text{Eq. 11}$$

Coming to the membrane heat transfer model, heat transfer through the membrane is partially due to membrane material and partially due to the vapor bubbles that reside in the membrane pores during transport. Their combined heat transfer coefficient is given as:

$$h_m = \frac{k_g \varepsilon + k_m(1 - \varepsilon)}{\delta} \quad \text{Eq. 12}$$

Latent heat of vaporization is an experimental factor and can be calculated using average bulk temperature and the relation.

$$\Delta H_v = 1.7535T + 2024.3 \quad \text{Eq. 13}$$

Mass Flux (J_w) can be calculated using partial vapor pressure on both sides of membrane and permeability coefficient of membrane material.

$$J_w = B_m(P_{mf} - P_{mp}) \quad \text{Eq. 14}$$

Partial pressures on both sides of membrane are calculated using Antoine's equation that relates a given temperature to vapor pressure as:

$$P^v = \exp\left(23.328 - \frac{3841}{T - 45}\right) \quad \text{Eq. 15}$$

Permeability coefficient (B) of membrane depends on the transport model used for vapors. A combination of Knudsen and molecular diffusion models has been reported as the most suitable option in literature for MD process. For that case, combined permeability coefficient (B_m^c) can be calculated as:

$$B_m^c = \left[\frac{3\tau\delta}{2\varepsilon r}\left(\frac{\pi RT}{8M}\right)^{\frac{1}{2}} + \frac{\tau\delta P_a RT}{\varepsilon PDM}\right]^{-1} \quad \text{Eq. 16}$$

Where P_a represents air trapped in the pores and D is coefficient of water diffusion. Water-air PD is given by:

$$PD = (1.895 \times 10^{-5})T^{2.072} \quad \text{Eq. 17}$$

At steady state,

$$Q_m = Q_f = Q_p = Q$$

Substituting values of coefficients in the above equation, we get:

$$Q = \left(\frac{1}{h_f} + \frac{1}{h_m + \frac{J_w \Delta H_v}{T_{mf} - T_{mp}}} + \frac{1}{h_p}\right)^{-1} (T_f - T_p) \quad \text{Eq. 18}$$

Overall heat transfer coefficient for transport model can be written as:

$$U = \left(\frac{1}{h_f} + \frac{1}{h_m + \frac{J_w \Delta H_v}{T_{mf} - T_{mp}}} + \frac{1}{h_p}\right)^{-1} \quad \text{Eq. 19}$$

Total heat transfer can then be simplified as:

$$Q_t = U(T_f - T_p)$$

This mathematical model is used to calculate the TPI in the research for evaluation of a combination of spacer arrangement and operating parameters.

3.2 Computational Model

A 2D computational domain is investigated in DCMD configuration for the scope of this project. 3 regions are made in xy plane using Design Modeler of commercial CFD tool ANSYS 2019 R3. Upper region is for Feed flow, lower one is the permeate channel while membrane is sandwiched between them. The model was checked for Mesh Independence before proceeding to setup and solution part using ANSYS FLUENT. Mathematical model for heat transfer in all three regions was used as base to calculate vapour flux. Temperature polarization index (TPI) is used as the dependent parameter to evaluate performance of a combination of design and operating parameters. Model was validated using the work of Shakib et al. [17] as reference.

3.2.1 Computational Domain

Analysis in this study is done on a selected computational domain where flow is developed, and spacers are implanted in feed and permeate channels.

3.2.1.1 Geometry

The domain under observation consists of two 38 mm long and 1 mm wide channels for feed and permeate. Membrane is a rectangular surface sandwiched between them of varying thickness. Geometry model is made using Design Modeler by making surfaces from sketches. Spacers in the model are made using Boolean function. Spacer filaments are circular in shape and distance among them is varied from 2 mm to 6mm. Filaments are distributed over mid 18 mm of the channels allowing the flow to develop in the initial region.

3.2.1.2 Nomenclature for Geometry

Geometry parameters are represented by letters as a guide for spacer arrangement and comparison of different combinations. Nomenclature used hereafter for geometry features is summarized in Table 1 below.

Table 1. Nomenclature Key Used in Study

Geometry Feature	Symbol
Feed Channel	F
Permeate Channel	P
Membrane	M
Wall	W

For spacer arrangement, combination of these letters and C for center is used. Multilayer spacer arrangement includes combination of any two among W, M and C to represent spacer arrangement as seen from Feed inlet side. For instance, in single spacer arrangement FWPM suggests that the spacer ii Feed channel (F) is placed along its Wall (W) and in Permeate Channel (P), it is along the Membrane (M). In case of multilayer spacer arrangements, FCMPMW represents an arrangement of spacers where the first spacer from feel inlet side is placed in Center (C) of feed channel while next spacer is on the membrane side. Similarly, on the permeate side, first spacer is along the membrane while next spacer is placed along the wall and same order is repeated throughout the computational domain. Geometry with FMPM arrangement is shown in fig-4 for reference.

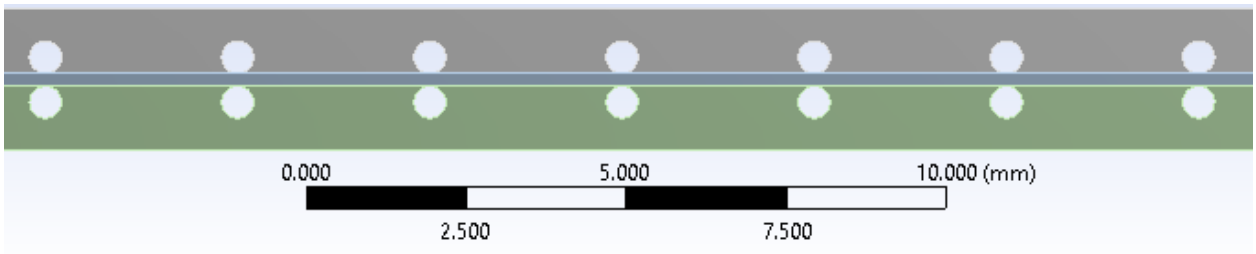

Figure 4. Computational Geometry with FMPM Spacers

3.2.1.3 Meshing

The geometry with spacers was imported to ANSYS Meshing to generate a Quadrilateral Dominant Mesh. Edge Sizing is used utilized with a biasing factor of 2 for membrane on lateral sides refining the mesh near membrane walls. Element size is used as the independent parameter to refine the mesh during Mesh Independence and further calculations.

Element Size of 0.1 mm, 0.075 mm, 0.05mm, 0.025 mm and 0.01 mm are tested for Mesh Independence of model. Meshes generated using the element sizes have been shown in fig-5. Temperatures at feed and permeate channel output, TPI and average temperatures on feed and permeate sides of membrane are taken as output parameters used to evaluate Mesh Independence.

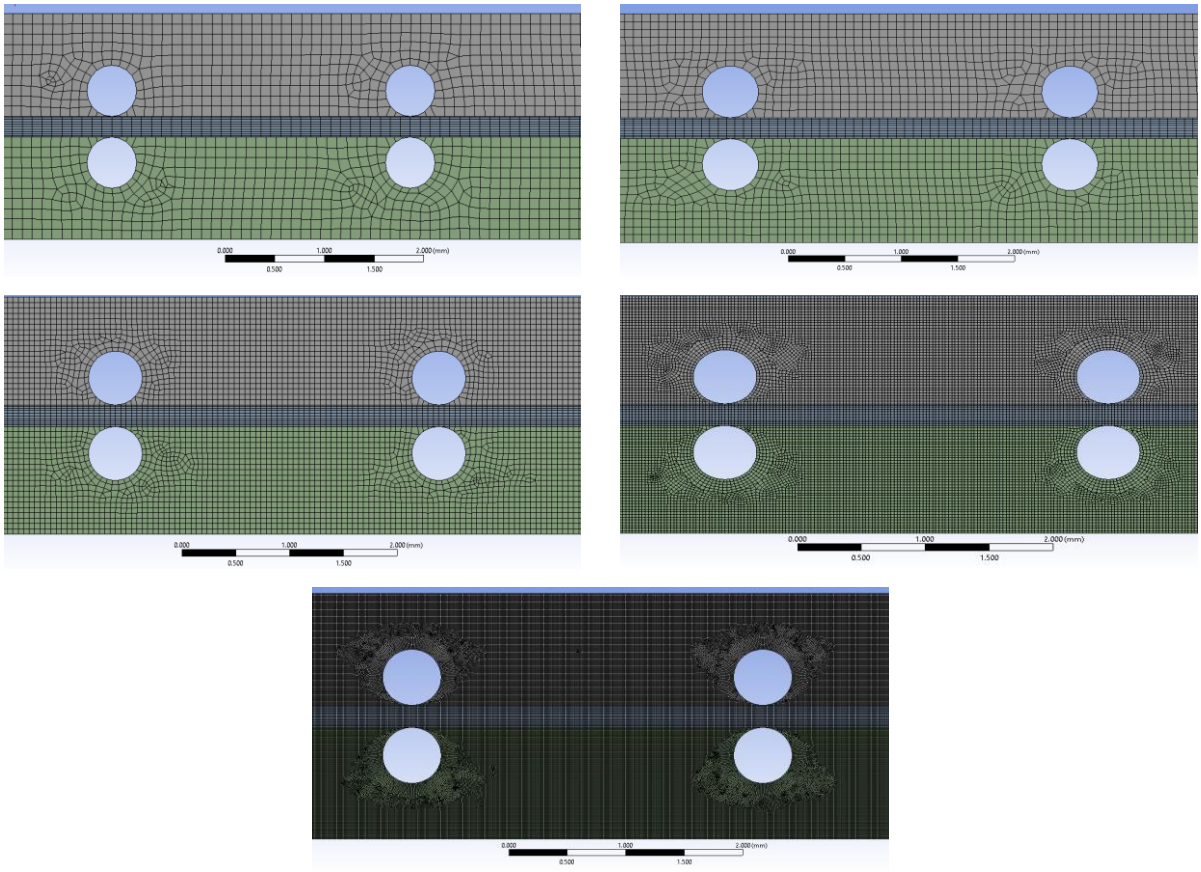

Figure 5. Mesh for Computational Solution. A) 0.1 mm B) 0.075 mm C) 0.05 mm D) 0.025 mm E) 0.01 mm

Named selections for inlet, outlet, and walls for both feed and permeate channels were made and later used to setup boundary conditions.

3.2.1.3 Numerical Solution

ANSYS FLUENT is used as the solver for this study. Spalart Allmaras and K Omega SST turbulence models are used for reference and current study, respectively. Pressure-Velocity coupling is coupled through SIMPLE (Semi-Implicit Method for Pressure Linked Equations) algorithm. Governing equations for momentum are solved through QUICK (Quadratic Upstream Interpolation for Convection Kinetics) solution scheme whereas Second Order Upwind scheme is used for Energy and Turbulence equations. Convergence criteria for convergence is set to 1×10^{-6} for Continuity, Velocity and Energy residuals. Physical properties of materials for membrane, feed and permeate channels are presented in Appendix.

Solution of the model is processed through CFD Post of ANSYS. Contours for temperature and velocity for the combinations under investigation are made using CFD Post. Temperature values on both sides of membrane are exported to calculate TPI at each point.

Temperatures at feed and permeate outlet are calculated using Average Area function calculator as required in Mesh Independence Study.

3.2.1.4 Calculations and Analysis

Calculations using the exported data from CFD Post is processed using Excel application of Microsoft Office 365.Calculation of Reynold Number, Prandlt Number, Nusselt Number, vapor pressures, and coefficients is automated using formulas in a single worksheet of Excel. Temperature polarization index is calculated and plotted using separate worksheet for every combination of geometry and operating parameter setup. Calculated instantaneous and average values are compared for different cases to determine the optimum combination.

3.2.2 Mesh Independence Study

Developed computational Model was inspected for mesh independence to ensure numerically valid solution. Mesh was refined using element size and exact same model was solved to check the solution dependence. Element sizes of 0.1 mm, 0.075 mm, 0.05 mm, 0.025 mm, and 0.01 mm are checked for the quality. Output parameters used to check independence are temperature at feed and permeate outlets, average temperature on both sides of membrane and calculated temperature polarization index of the computational domain.

Mesh Independence was studied for 4 different spacer arrangements, Trend of temperatures for FMPM and FMPW arrangement is presented in fig-6 and fig-7 respectively.

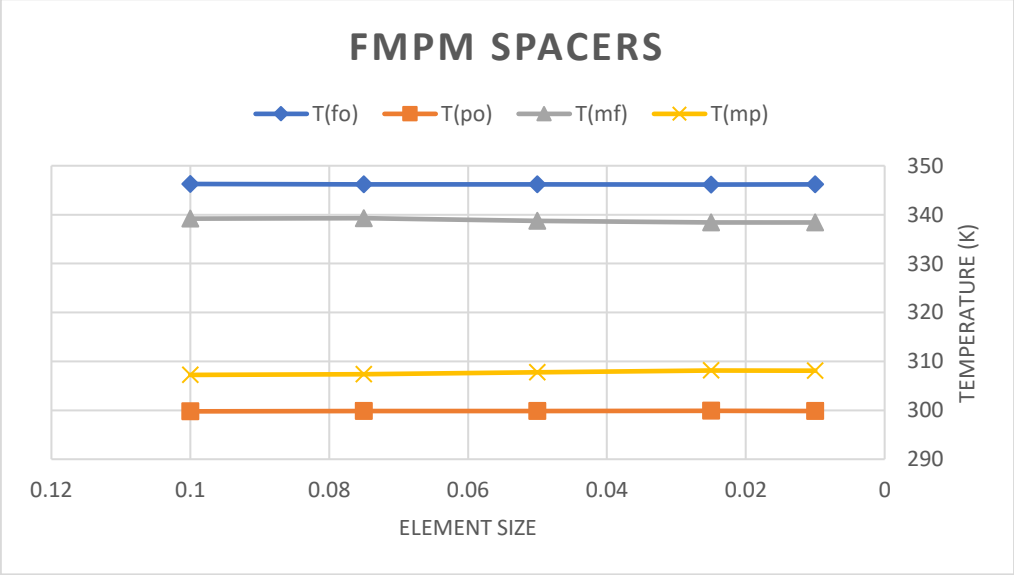

Figure 6. Relation of Temperatures Mesh Element Size for FMPM Spacers

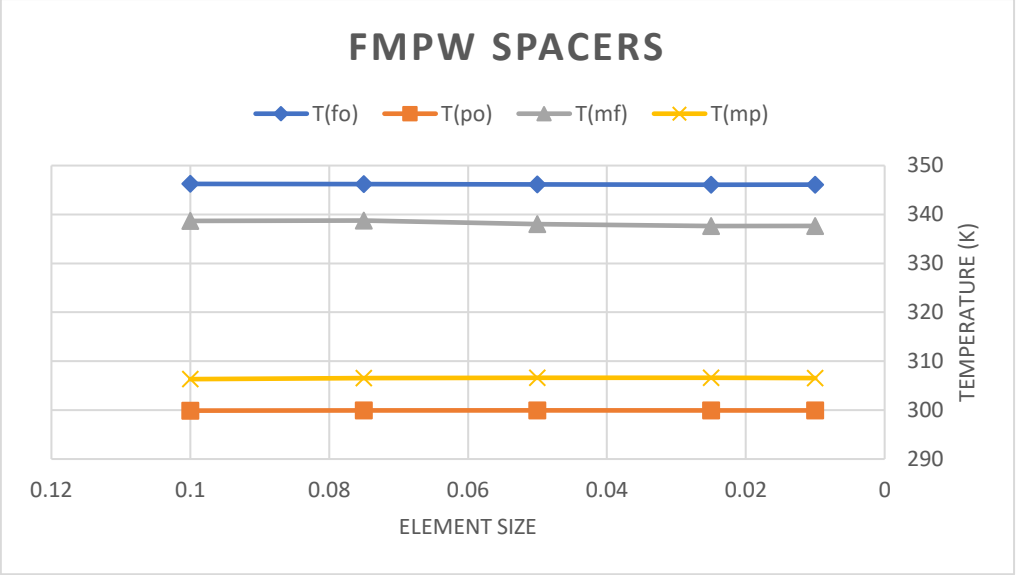

Figure 7. Relation of Temperatures Mesh Element Size for FMPW Spacers

Similarly, TPI trend for FWPM and FWPW spacers is given in fig-8 and fig-9.

As a result of this trend and time for computation, mesh element size of 0.025 mm is used in the research.

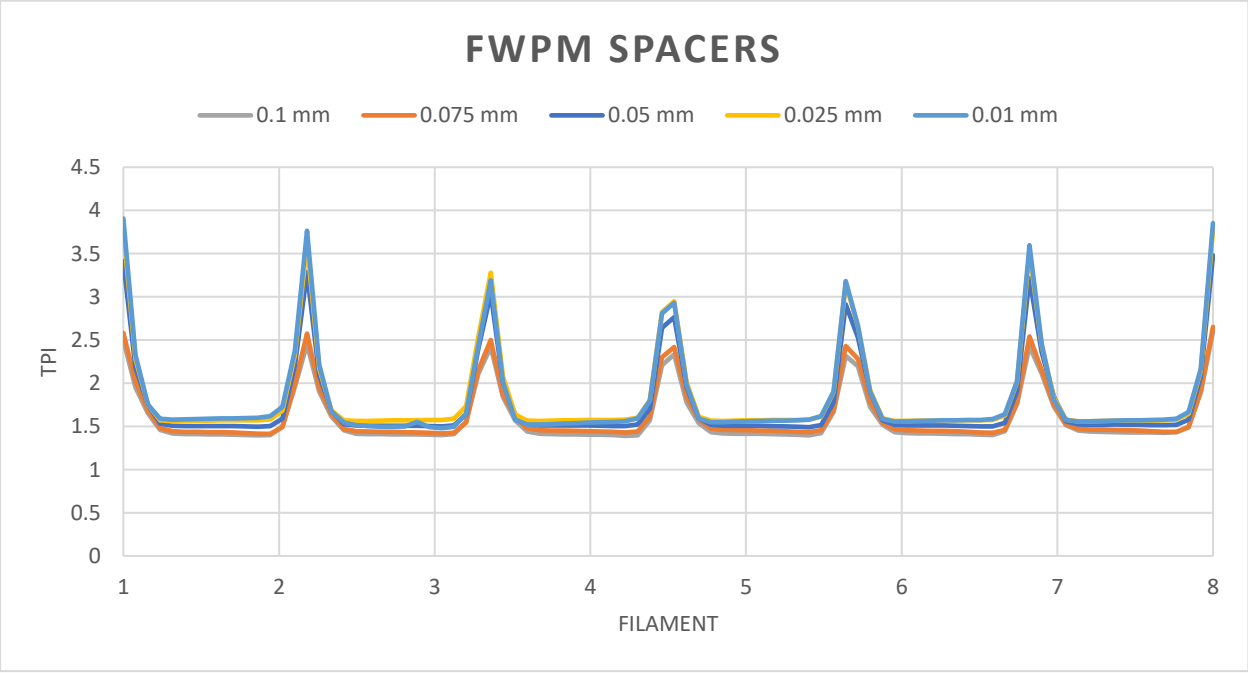

Figure 8. Relation of Temperatures Mesh Element Size for FWPM Spacers

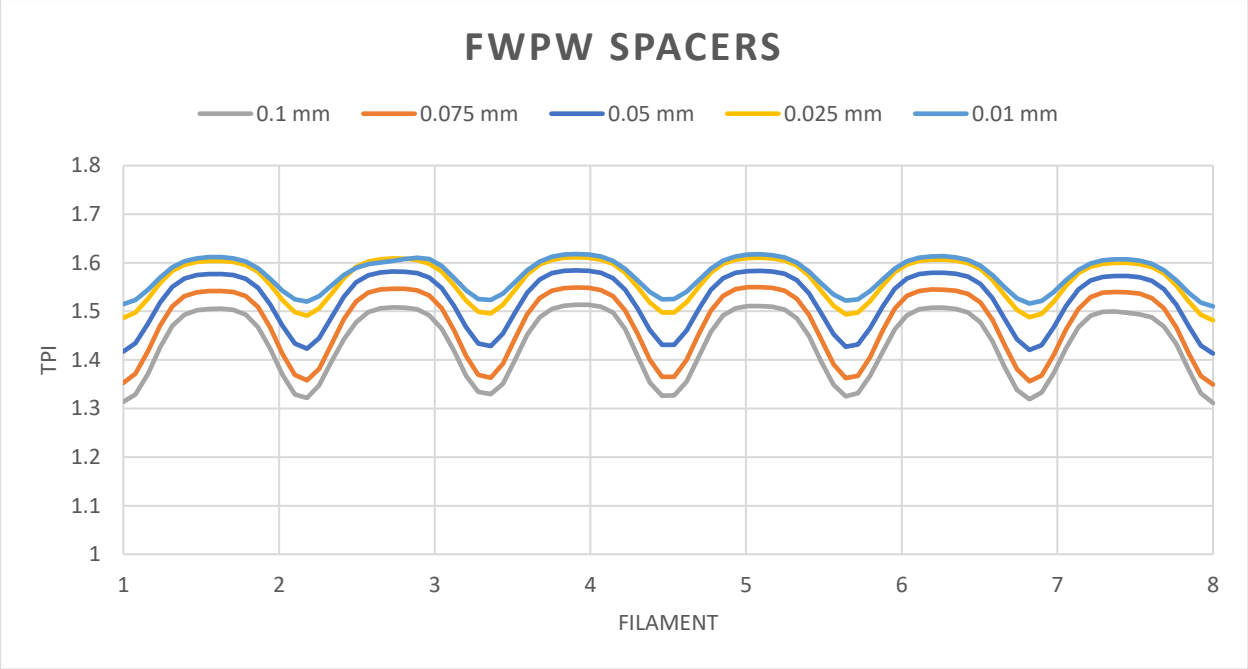

Figure 9. Relation of Temperatures Mesh Element Size for FWPM Spacers

3.2.3 Model Validation

The computational model developed for the study has been validated using the work of Khalifa et al. [17]. They have validated the model experimentally and by reproducing their results for two different cases in their work, the current computational model is validated. Several geometry arrangements are studied the reference work, cases CI45 and AS45 have been recreated in this study. Temperature and velocity contours along with temperature distribution on the at the reference points and their resultant TPI have been used as the validating factors.

Temperature contours for CI45 case in reference paper and present work are given in fig-10. Similar trend as well as similar values of temperatures can be observed in fig-11 as well where temperature distribution along the length of computational domain has been recreated successfully with 3 reference filaments.

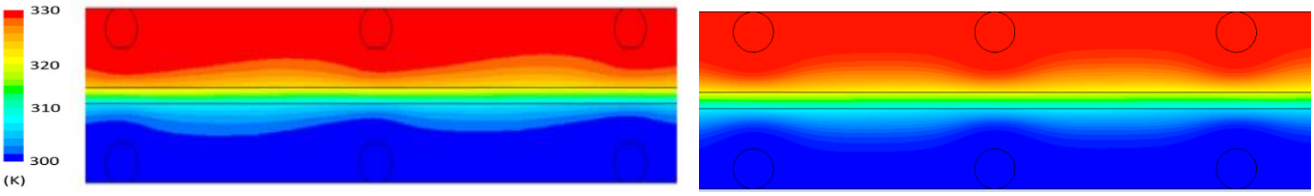

Figure 10. Temperature Contours for CI45 case A) Experimental B) CFD Model

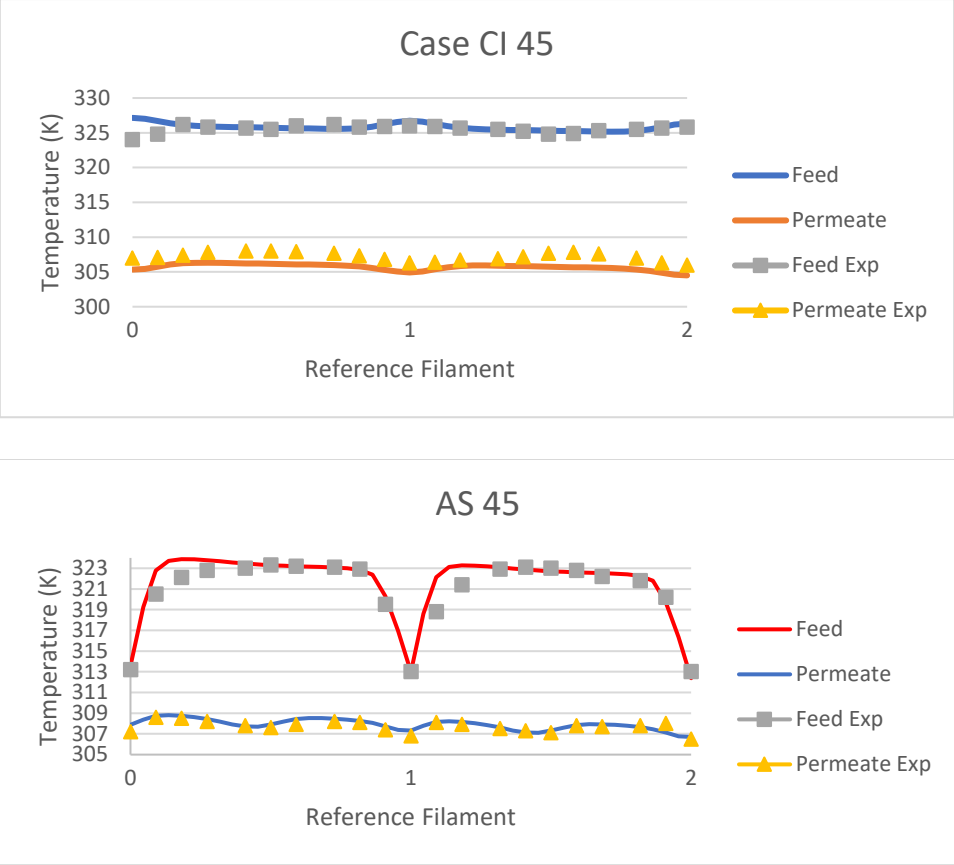

Figure 11. Temperature Distribution A) CI45 case recreated B) AS45 case recreated

Similar values were obtained for the same cases using two different turbulence models. Based on matching trends and similar values obtained, the validated model is used for further study and analysis.

3.2.4 Model Setup

Loaded mesh contains three different cell zones. Feed and permeate channels are selected as fluid zones with brine solution in feed and liquid water in permeate side assigned for flow. Membrane material is created by assigning the properties of commercially available hydrophobic membrane material and a constant heat flux of 0.2 W/m^2K for heat transfer across the membrane. Spalart Allmaras (SA) turbulence model is used in the reference paper, similar values are obtained using K Omega SST turbulence model that provides better results for reference paper. To have a better look at the effect of various parameters and owing to availability of computation power, K Omega SST model is used in this research.

Named selections made during meshing are used to define boundary conditions. Both sides of membrane and the walls of feed and permeate channel mating membrane sides are defined as interfaces to model heat transfer. Inlets for both channels are given velocity and

temperature values. No slip boundary condition is implemented at walls of geometry. Outlets for both channels are given pressure outlet boundary conditions. Convergence values for residuals of Energy, Turbulence, Velocity and Continuity are set as 1×10^{-6}.

Pressure Velocity coupling for solver is done using SIMPLE (Semi Implicit Methods for Pressure Linked Equations) scheme with higher order QUICK (Quadratic Upstream Interpolation for Convection Kinetics) method used for momentum equations whereas Second order Upwind models are used to solve energy and Turbulence governing equations. Solution is exported to CFD Post module of ANSYS to calculate average temperatures and export the values of temperature at selected computational domain to calculate TPI and determine the optimum conditions.

Chapter 4: Results and Discussion

Effect of spacers configuration as well as other operational parameters has been studied in this project. Results of CFD study are presented in this chapter.

4.1 Effect of Membrane Thickness

Membrane thickness of 0.15 mm, 0.175 mm and 0.2 mm are tested at same operating conditions of velocities, temperatures and boundary conditions using same geometry with spacers in FWMPWM configuration with inter-filament distance of 3mm. Effect of varying membrane thickness on TPI is presented in fig-12 and average values tabulated in Table 2..

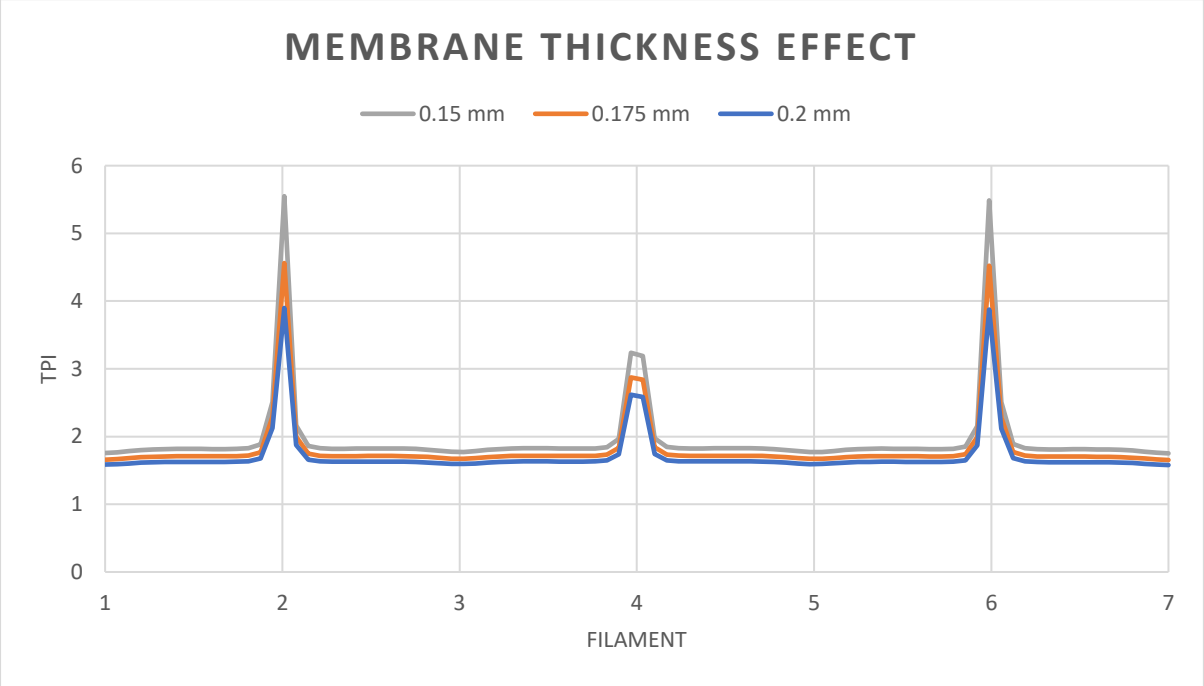

Figure 12. Effect of Membrane Thickness on TPI

Table 2. Average TPI values for varying Membrane thickness

Membrane Thickness	0.15 mm	0.175 mm	0.2 mm
Average TPI	1.9532	1.8160	1.7145

Average TPI value decreases as we increase the membrane thickness due to increased heat transfer area through conduction. In addition to increased heat transfer, mass transfer resistance is also increased. Increased resistance to mass transfer arises as some vapors get stuck in the membrane pores and block the passage for incoming vapors. A compromise between area for heat transfer and mass transfer resistance is used to select the ideal membrane for each case. In this study, membrane thickness of 2 mm is used for further cases.

4.2 Effect of Velocity

Effect of velocity on MD effectiveness has been widely studied. Effect of velocity is recreated here to study the combination of operating parameters for an optimum setup. Inlet velocities for both Feed and Permeate channels were varied from 0.01 ms^{-1} to 0.35 ms^{-1} in FWPW configuration of spacers with 3mm distance among filaments. Results are presented in fig-13 and Table 3 below.

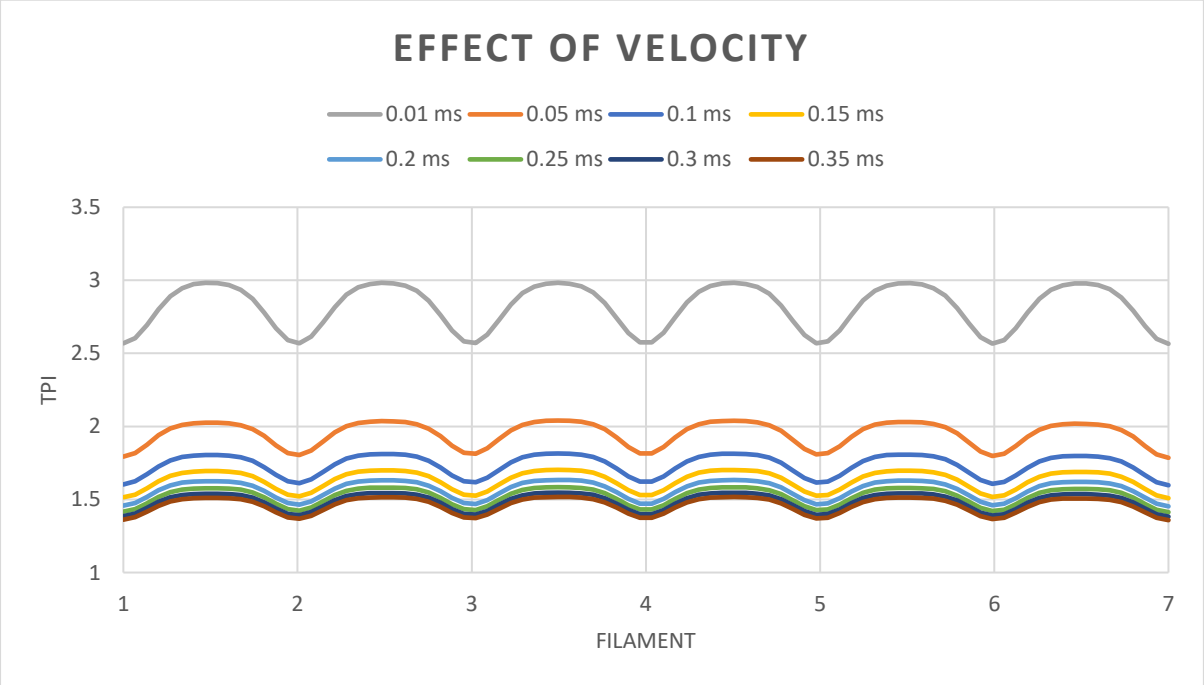

Figure 13. Effect of Velocity on TPI

Table 3. Average TPI values for varying Velocity

Velocity	0.01	0.05	0.1	0.15	0.2	0.25	0.3	0.35
Average TPI	2.8158	1.9473	1.7344	1.6321	1.5680	1.5226	1.4880	1.4604

Average TPI is decreased as velocity is increased. Same agrees with literature available on the subject. Higher velocity results in higher shear stress on the membrane walls. This in turn increases turbulence in feed stream leading to better heat transfer thus lower TPI.

4.3 Effect of Spacers

To study the effect of spacers, it is important that we study the performance of the MD setup without spacers. Validated model is recreated without the spacer using same operating conditions. The result of no spacer case is presented in fig-14- below.

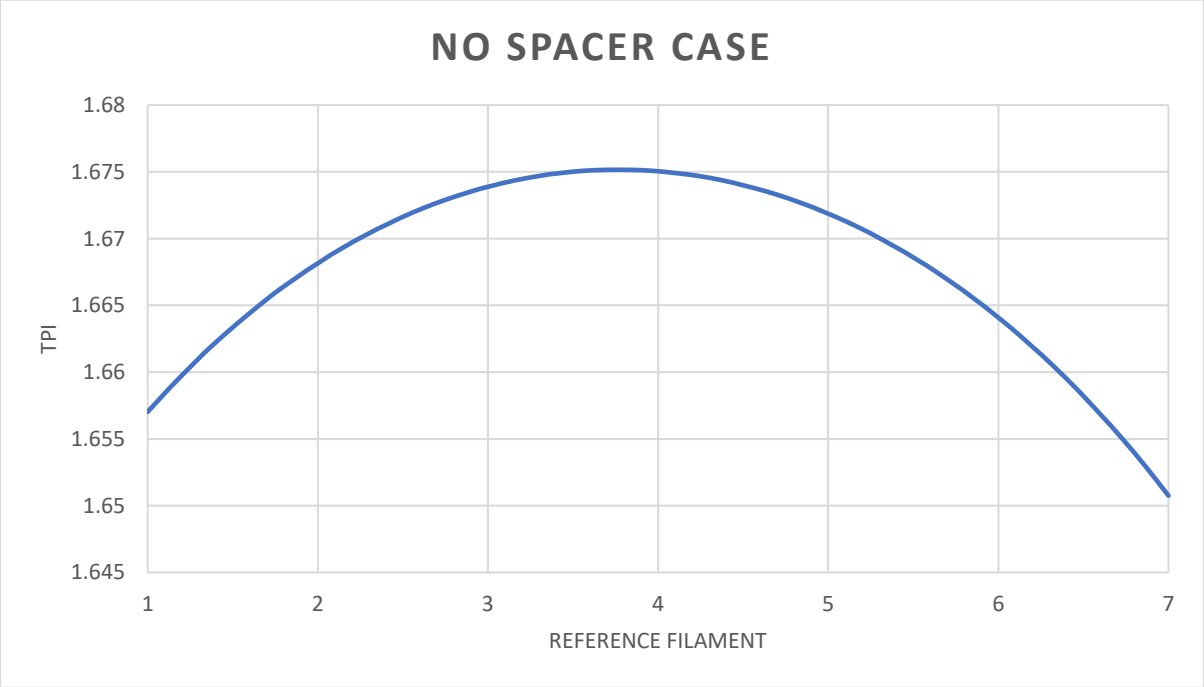

Figure 14. No spacer Case for TPI

Average TPI value for this case comes out to be 1.6681. highest value of TPI can be seen in the middle of channel. This is due to the lowest temperature difference at that point. Feed channel gets cooler as it goes from left to right and permeate solution gets hotter as it passes from right to left. Lower TPI value on right side of graph than the left side is due to lower difference of permeate inlet and feed outlet temperature than that of feed inlet and permeate outlet. This case is taken as reference to study the performance of spacer filled channels in various arrangements.

Effect of spacers is studied considering filament size, inter filament distance and their arrangement in feed and spacer channels. Results are presented one by one.

4.3.1 Effect of Spacer Filament Size

Spacers under investigation are of circular cross section and their variants of 0.25 mm, 0.50 mm and 0.75 diameter for a single filament are considered. Effect of spacer size is studied in a single layer as well as multilayer spacer arrangements. Average TPI values as well as its distribution for different cases are presented in tables 4,5 and fig-15 to fig-19 below.

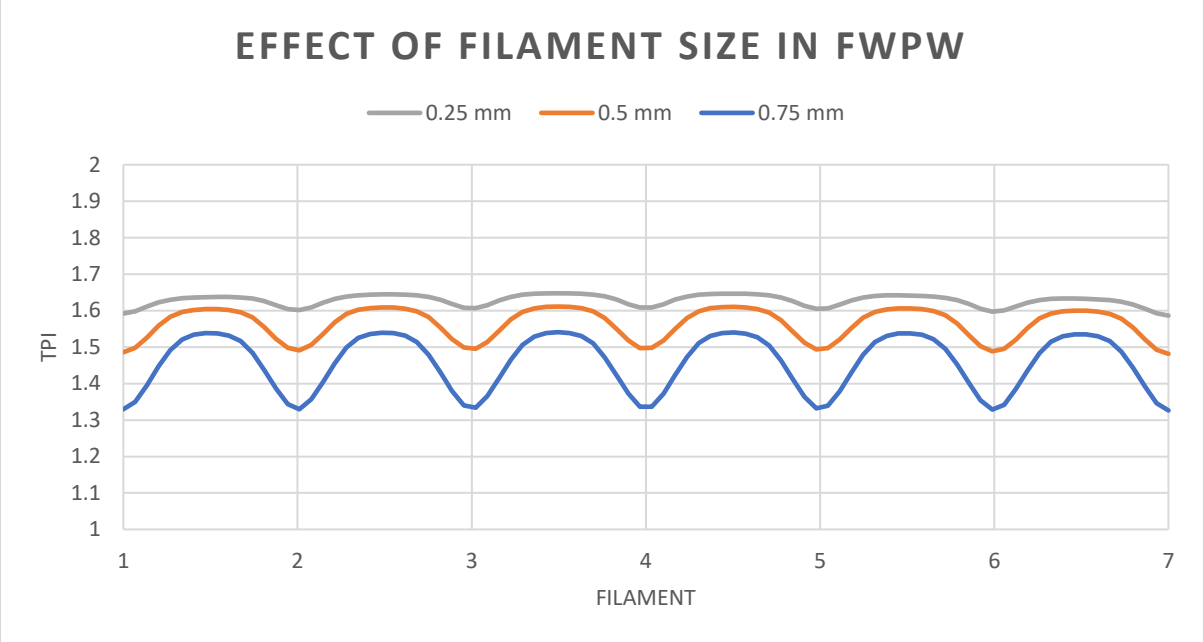

Figure 15. Effect of Filament Size on TPI for FWPW Single Layer Spacer

Table 4. Average TPI values for varying Filament Size in FWPW

Filament Size	0.25 mm	0.5 mm	0.75 mm
Average TPI	1.9532	1.8160	1.7145

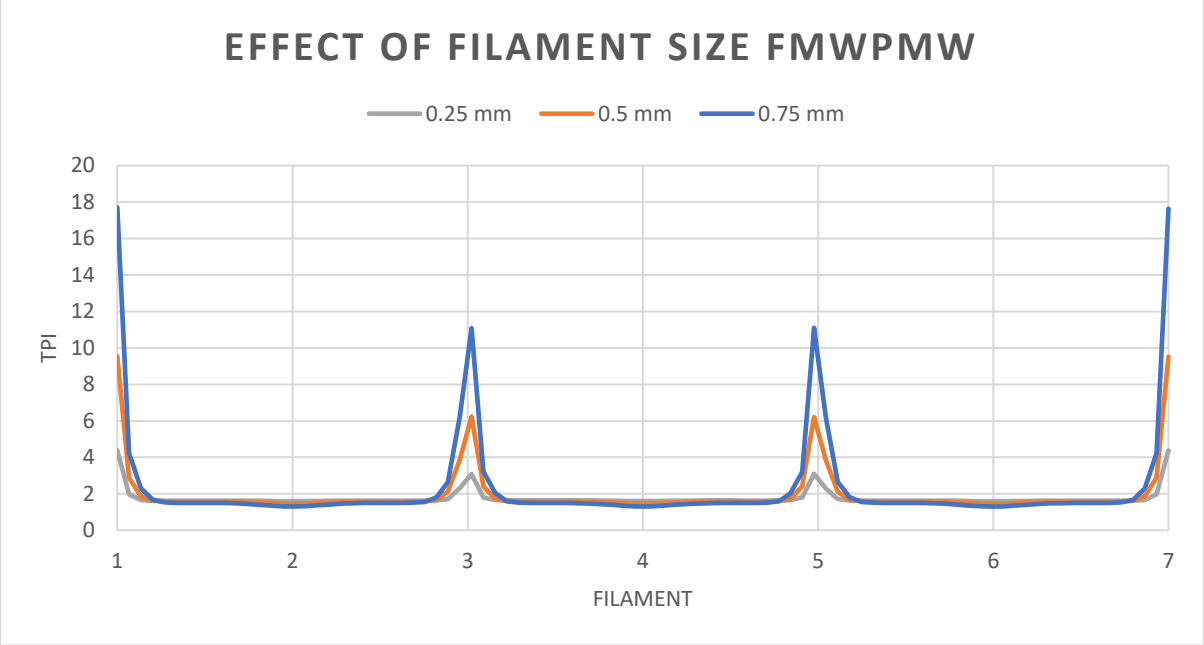

Figure 16. Effect of Filament Size on TPI for FMWPMW Multi-Layer Spacer

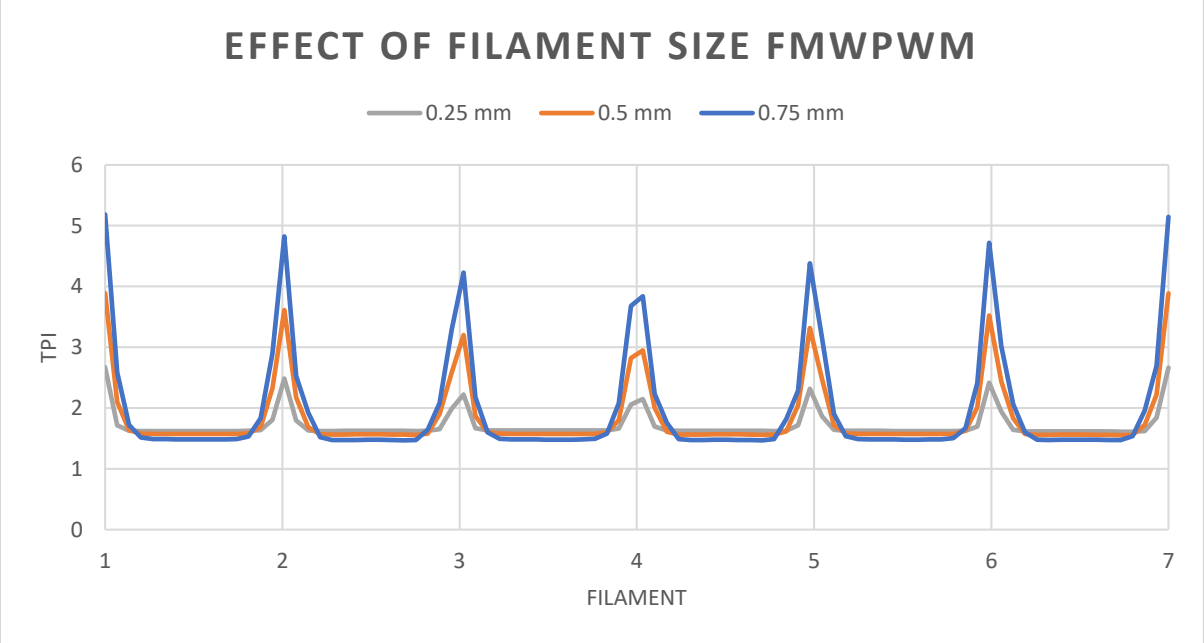

Figure 17. Effect of Filament Size on TPI for FMWPWM Multi-Layer Spacer

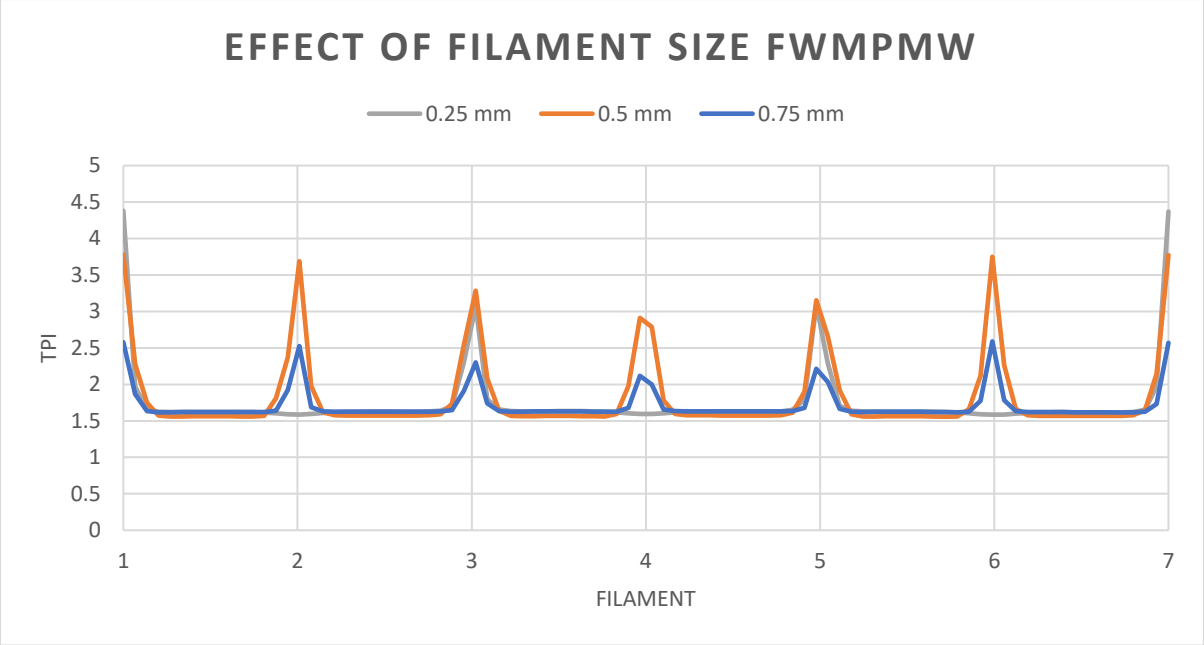

Figure 18. Effect of Filament Size on TPI for FWMPMW Multi-Layer Spacer

Table 5. Average TPI values for varying Filament Size in Multi-Layer Spacers

Spacer Arrangement	**Filament Size**	0.25 mm	0.5 mm	0.75 mm
FMWPMW	**Average TPI**	1.7430	1.9598	2.3036
FMWPWM		1.7125	1.8275	1.9516
FWMPMW		1.7430	1.8274	1.7126
FWMPWM		1.7145	1.8767	2.1277

It is evident that average TPI value is higher in multilayer spacer arrangements that in a single layer spacer arrangement. Highest average value is observed in case of FMWPMW arrangement with a spacer diameter of 0.75 mm.

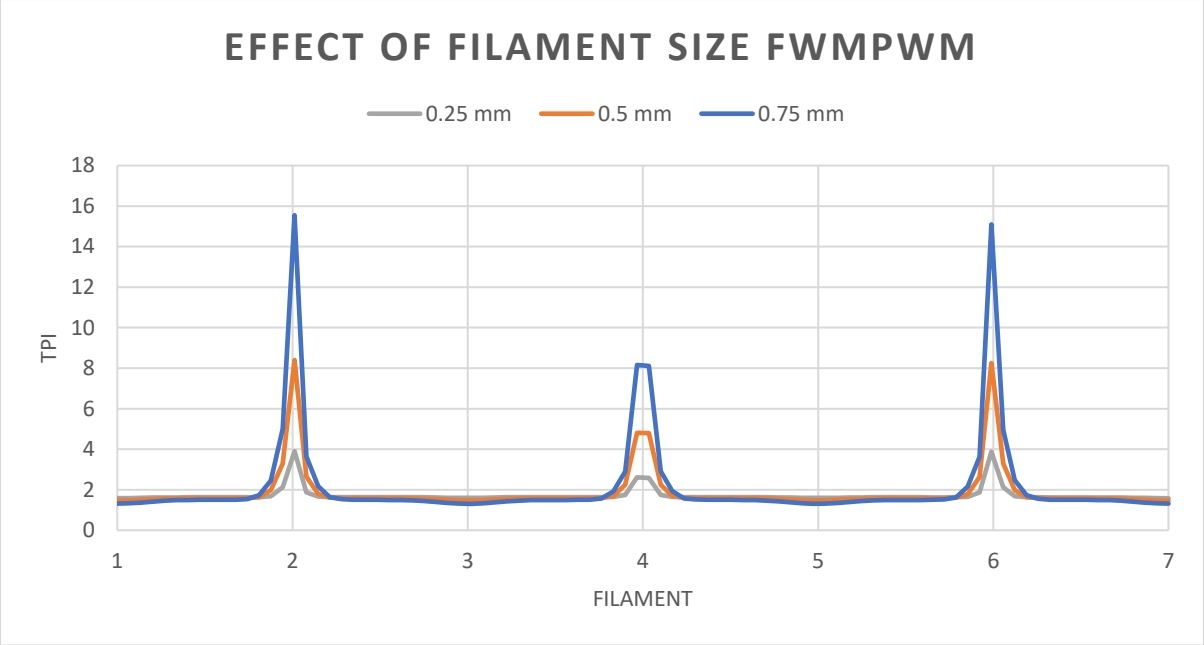

Figure 19. Effect of Filament Size on TPI for FWMPWM Multi-Layer Spacer

Average TPI increases as the spacer size increase for multilayer arrangements while it decreases with increasing spacer size in single layer spacer arrangement. Reason behind this inverse behaviour is that for single layer spacer, turbulence causes enhanced mixing and heat transfer thus producing lower TPI values. In case of multilayer spacer arrangement and increased spacer diameter, turbulence generated is too much and does not allow the stream to flow properly thus hindering the heat transfer and effective contact area for vapors to flow through the membrane. This hinderance produces higher TPI values making larger filament size unfavorable in multilayer spacer arrangement.

While for single layer spacers, larger filament size produces better results. Spacer diameter of 0.5 mm is selected for rest of the study to compare the results of different combinations using a common set up and same operating conditions.

4.3.2 Effect of Spacer Inter-Filament Distance

Spacer filaments in the computational domain are distributed over 18 mm in the middle of feed and spacer channels. Center to center spacer filament distance of 2 mm, 3 mm, 4.5 mm, and 6 mm is tested in this study.

Effect of inter-filament distance for FWPM arrangement is tabulated and presented in table 6 and fig-20 below. It can be observed that as inter filament distance increases, average

TPI value decreases depicting better performance. When the obtained values are compared with no spacer case, all of them are higher than average TPI of reference case.

Net type spacers are available commercially of varying filament spacing. To compensate for all possible spacer arrangements in the study, filament distance of 3 mm resulting in 6 filaments to be arranged varyingly is selected.

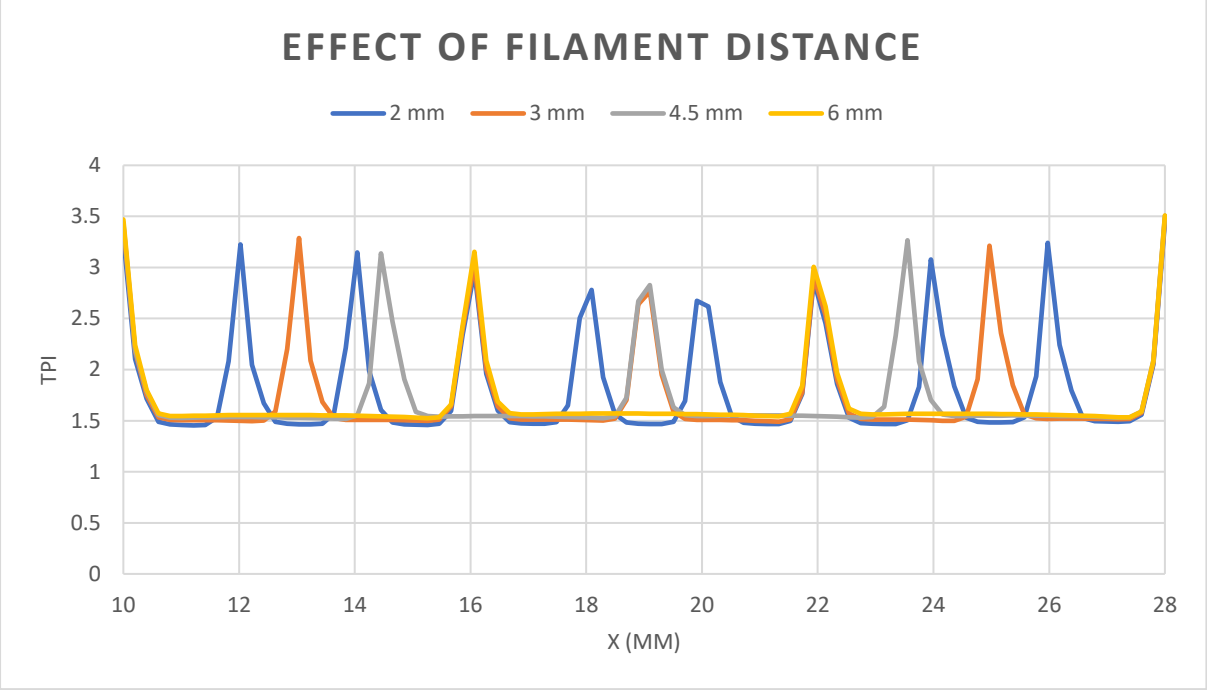

Figure 20. Effect of inter-filament distance on TPI for FWPM spacer

Table 6. Average TPI values for varying inter-filament distance

Filament Distance	2 mm	3 mm	4.5 mm	6 mm
Average TPI	1.8152	1.7481	1.7082	1.6884

4.3.3 Effect of Spacer Filament Arrangement

Spacer filaments can be arranged on membrane side, wall side or suspended mid channel for both feed and permeate channels. Different combinations of all these arrangements are tested in the study to find the optimum arrangement keeping the same operating conditions and model setup.

4.3.3.1 Single Layer Spacer Arrangements

4 different arrangements of spacers aligned in feed and permeate channels are tested. They are named as FMPM, FMPW, FWPM and FWPW representing the position of spacer in feed and permeate channels.

Effect of including single layer of spacers in feed and permeate spacers is presented in fig-21 and average value for each variation in table 7. By adding spacers on membrane side produces negative effects and TPI is increased by many folds. Best result is obtained when spacer layer is placed away from membrane. Infact it is the only arrangement where obtained TPI value is better than no spacer arrangement.

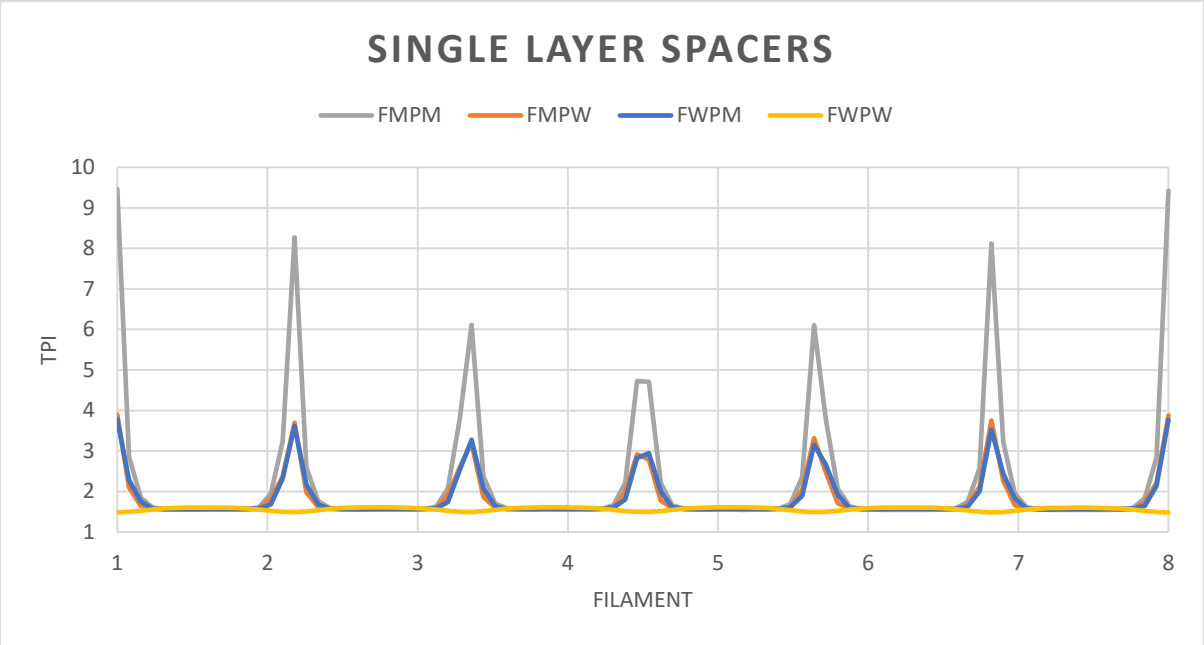

Figure 21. Effect of Single Layer Spacer on TPI

Table 7. Average TPI values for Single Layer Spacer arrangements

Spacer Arrangement	FMPM	FMPW	FWPM	FWPW
Average TPI	2.2620	1.8268	1.8286	1.5633

Putting spacer layer adjacent to membrane layer increases the temperature difference and providing more resistance to mass transfer by covering membrane pores in the surrounding.

When spacers are placed away from membrane, they produce turbulence in the flow causing increased mixing and shear stress thus resulting in better TPI.

4.3.3.2 Multi-Layer Spacer Arrangements

Spacers can also be arranged in multiple layers. Considering the filament size of 0.5 mm, spacer layers cannot be arranged exactly aligned one above the other as it will block the flow in respective channels. Using the results of reference paper where staggered arrangement of spacers was found to be more effective, staggered arrangements of multiple layers of spacers is investigated and results are presented in fig-22 with average values presented in table 8 below.

In staggered arrangement, there is possibility of having spacers on both sides of the membrane at an instance and away from membrane on both sides at another location as in case of FMWPMW and FWMPWM arrangements. In addition to that, possibility of having spacer filament on only one side of membrane is also incorporated in case of FMWPWM and FWMPMW arrangements.

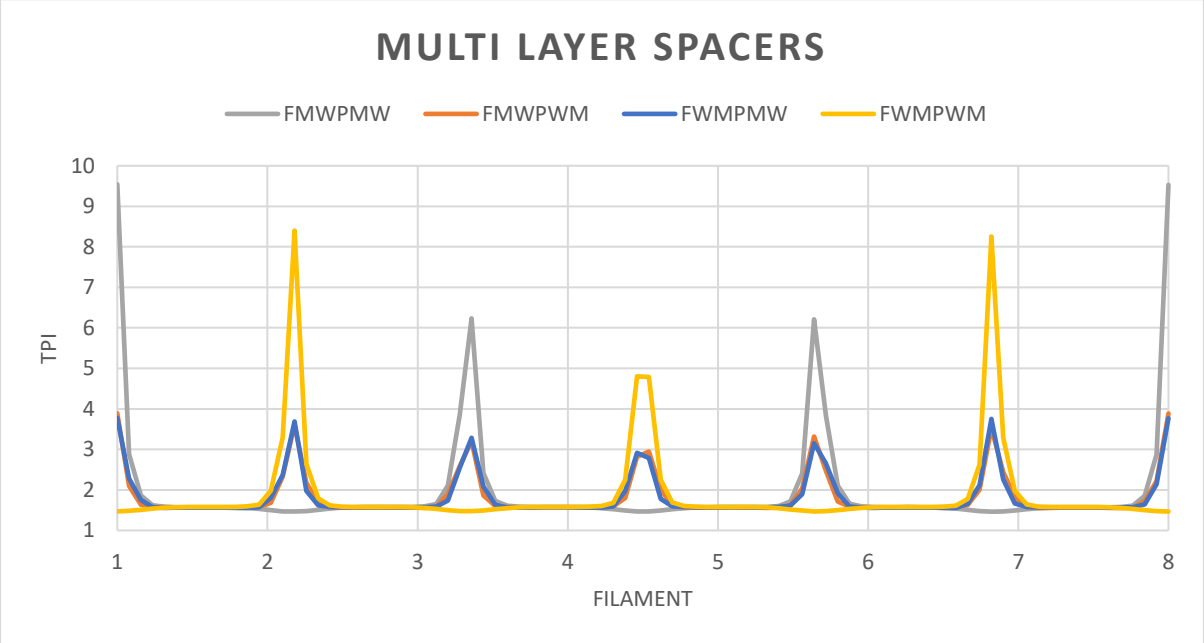

Figure 22. Effect of Multi-layer Staggered Spacers on TPI

Table 8. Average TPI values for Multi-Layer Spacer arrangements

Spacer Arrangement	FMWPMW	FMWPWM	FWMPMW	FWMPWM
Average TPI	1.9598	1.8275	1.8274	1.8767

TPI is observed highest when spacer filaments are present on both sides of membrane. Average value of TPI is lower for FWMPWM than in FMWPMW due to location of first adjacent filament on both sides of membrane. For FWMPWM, the flow interacts with wall filament first thus increasing the velocity for interaction with filament on membrane side. This increased velocity causes lower TPI value in the said case. Similar results are observed for other two cases where only one filament is attached to membrane at any time.

Velocity contours of FMWPMW arrangement with a filament size of 0.75 mm is shown in fig-23. It is observed that for larger filament in multi-layer spacers, flow is not developed as much to impact the results.

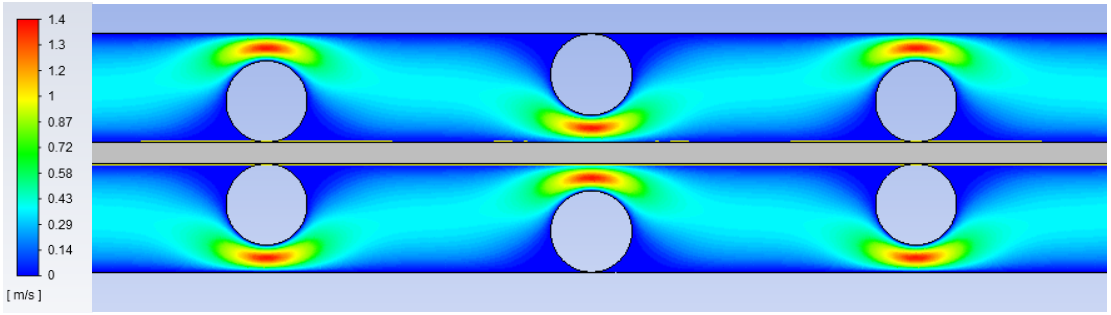

Figure 23. Velocity Contours for FMWPMW spacer with 0.75 mm diameter

Considering the effect of filament size in multilayer spacers as discussed in section 4.3.1, better results are obtained for a combination of multilayer spacers with smaller filament size of 0.25 mm.

4.3.3.3 Center Mounted Spacer Arrangements

Another possible spacer arrangement is when none of spacer filament is in contact with either membrane or the wall of feed or permeate channel. Five such arrangements are also taken into consideration while finding the optimum combination. Spacer filaments are mounted in the center of flow channels. Combinations of spacer mounted mid channel on one side while being in contact with wall or membrane on the other side are also testing making five possible arrangements for this case. Comparison of TPI values for these arrangements along with average values is presented in fig-24 and table 9, respectively.

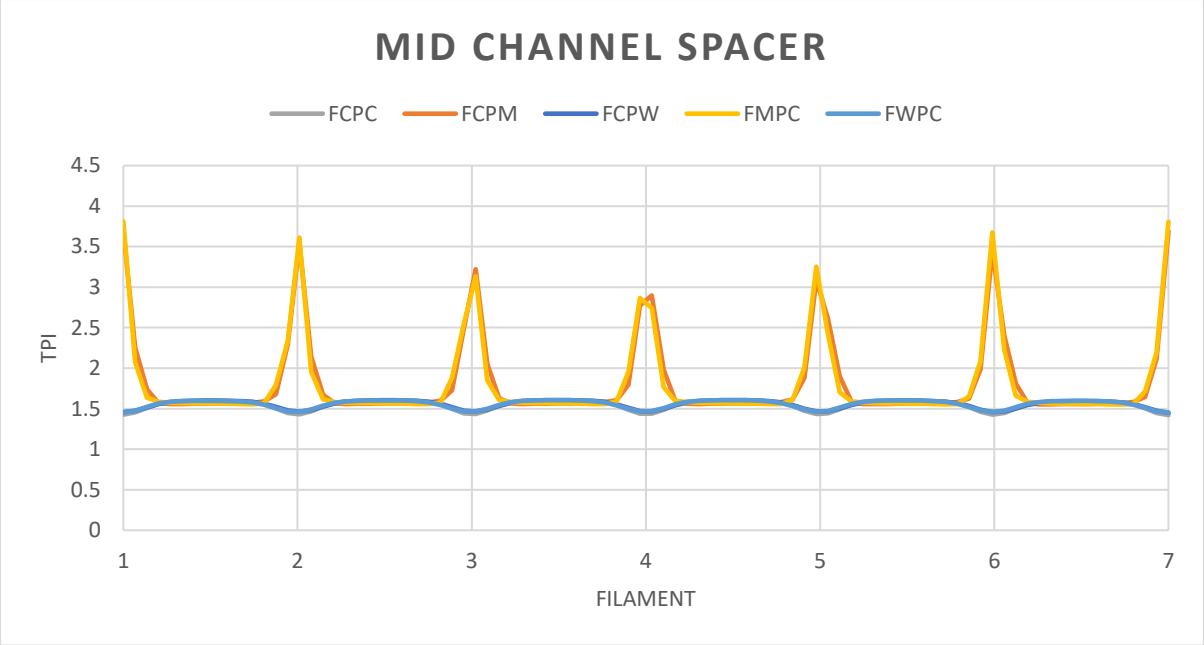

Figure 24. Effect of Mid Channel Spacers on TPI

Table 9. Average TPI values for Mid Channel Spacers

Spacer Arrangement	FCPC	FCPM	FCPW	FMPC	FWPC
Average TPI	1.5468	1.8163	1.5553	1.8132	1.5546

TPI values are highest for the arrangements when spacer filaments are placed on either side of membrane i.e. FCPM and FMPC. Results are similar for cases of FCPW, FWPC and FCP are similar with FCPC producing the lowest TPI values of all the arrangements tested.

Considering the effect of filament size in single layer spacers as discussed in section 4.3.1, better results are obtained for spacers with larger filament size. FCPC with filament size of 0.75 mm produces average TPI value of 1.4502.

Chapter 5: Conclusion and Future Work

Performance of a DCMD setup for water desalination using spacers in feed and permeate channels is investigated to find the optimum combination using CFD. Effect of velocity and membrane thickness is also incorporated to get the optimum combination of operating parameters and spacer geometry. Temperature Polarization Index is used as the evaluation parameter while using the values of no spacer case as reference.

It is concluded that best performance of a DCMD module can be obtained by adding single layer circular spacers mounted in the middle of feed and permeate channels. Higher inlet velocity of feed and permeate solutions increases the permeate flux as well as thicker membranes. Analyzing the performance of various spacer arrangements of varying spacer filament size, the best results are obtained for center mounted spacer of 0.75 mm diameter.

Single and multi-layer spacer arrangements produced different results for combination of operating parameters. Performance of DCMD setup with single layer spacers in feed and permeate channel is enhanced by increasing the temperature difference across membrane sides. Larger filament size produces better results in single layer whereas opposite trend is observed in multi-layer spacers. As we increase the spacer filament size in multi-layer arrangement, the temperature difference reduces and thus permeate production is halted.

An ideal combination of MD configuration can be concluded to possess high inlet velocities for feed and permeate solutions. Inlet velocity is limited by Liquid Entry Pressure (LEP) of hydrophobic membrane. Very high velocity will induce greater pressure on membrane surface. When this pressure exceeds LEP, water molecules make their way to permeate side along with vapors by destroying membrane pores.

Future of human race on earth greatly depends on availability of freshwater and desalination is the best possible solution to this challenge now. Further research to understand and improve DCMD as well as other MD configurations to meet the ever-increasing demand of freshwater. Another advantage of MD is its application in industrial water retreatment. Industries count for a good portion of water consumption, especially in developed countries. Retreating and reusing water can save major portion of water dumped into oceans and rivers damaging aquatic life and wasting usable resource.

Technology has allowed us to utilize our resources in an intelligent way by using CFD techniques and simulating our flow problems. Owing to limited computational power, K Omega turbulence model is used in this study. Higher order CFD simulations for DCMD are suggested to better understand the underlying phenomenon considering temperature as well as concentration polarization in combination. Higher order simulations will reveal more details and will help to improve the phenomenon.

Similar studies for other MD configurations should also be explored. Combination of Membrane Desalination and Reverse Osmosis can be particularly useful for processing of seawater with higher salinity like Arabian Sea which is also the major source of water for Pakistan. Another bright aspect to look deeper into is the integration of solar power with MD. Major energy consumption of MD is heat required to heat the feed solution, which can be provided by solar collectors. This combination can lead to fully solar powered desalination units specifically for remote areas with limited access to clean water or power.

MD applications are not limited to water desalination, its applications are found in medical field as well. Dialysis is a common procedure mandatory for kidney patient after a certain level of disease. Currently, medical devices for dialysis are imported in Pakistan. Hemodialysis is the most common type, and its working principle is based on MD where blood of patients is purified using a membrane module. Clean water from RO plant is used in this process to balance the electrolytes and necessary mineral content. Studying the process and exploring it in depth can lead to local manufacturing of these filters impacting lives of thousands of patients.

Chapter 6: References

[01] Matt Williams 2014, *What percent of Earth is water?*, Phys.org, <https://phys.org/news/2014-12-percent-earth.html>

[02] Howard Perlman 2019, *All of Earth's water in a single sphere!*, USGS, <https://www.usgs.gov/media/images/all-earths-water-a-single-sphere>

[03] Rutger Willem Hofste, Paul Reig and Leah Schleifer 2019, *17 Countries, Home to One-Quarter of the World's Population, Face Extremely High Water Stress*, World Resources Institute, <https://www.wri.org/blog/2019/08/17-countries-home-one-quarter-world-population-face-extremely-high-water-stress>

[04] IMF Staff Team 2015, *Issues in Managing Water Challenges and Policy Instruments: Regional Perspective and Case Studies*, <https://www.imf.org/external/pubs/ft/sdn/2015/sdn1511tn.pdf>

[05] Sehrish Wasif 2016, *Pakistan may run dry by 2025: study*, The Express Tribune, <https://tribune.com.pk/story/1112704/pakistan-may-run-dry-2025-study>

[06] Weyl, P.K., Research Corp, 1967. *Recovery of demineralized water from saline waters*. U.S. Patent 3,340,186.

[07] Singh, R.P., 2013. Water Desalination" The Role of RO and MSF". *IOSR Journal of Environmental Science, Toxicology And Food Technology (IOSR-JESTFT)*, *6*(2), pp.61-65.

[08] Ng, K.C., Thu, K., Kim, Y., Chakraborty, A. and Amy, G., 2013. Adsorption desalination: an emerging low-cost thermal desalination method. *Desalination*, *308*, pp.161-179.

[09] Greenlee, L.F., Lawler, D.F., Freeman, B.D., Marrot, B. and Moulin, P., 2009. Reverse osmosis desalination: water sources, technology, and today's challenges. *Water research*, *43*(9), pp.2317-2348.

[10] Fritzmann, C., Löwenberg, J., Wintgens, T. and Melin, T., 2007. State-of-the-art of reverse osmosis desalination. *Desalination*, *216*(1-3), pp.1-76.

[11] Pearce, G., Talo, S., Chida, K., Basha, A. and Gulamhusein, A., 2004. Pretreatment options for large scale SWRO plants: case studies of OF trials at Kindasa, Saudi Arabia, and conventional pretreatment in Spain. *Desalination*, *167*, pp.175-189.

[12] Service, R.F., 2006. Desalination freshens up.

[13] Lawson, K.W. and Lloyd, D.R., 1997. Membrane distillation. *Journal of membrane Science*, *124*(1), pp.1-25.

[14] Meindersma, G.W., Guijt, C.M. and De Haan, A.B., 2006. Desalination and water recycling by air gap membrane distillation. *Desalination*, *187*(1-3), pp.291-301.

[15] Alklaibi, A.M. and Lior, N., 2005. Membrane-distillation desalination: status and potential. *Desalination*, *171*(2), pp.111-131.

[16] Shirazi, M.M.A. and Kargari, A., 2015. A review on applications of membrane distillation (MD) process for wastewater treatment. *J. Membr. Sci. Res*, *1*, pp.101-112.

[17] Drioli, E., Ali, A. and Macedonio, F., 2015. Membrane distillation: Recent developments and perspectives. *Desalination*, *356*, pp.56-84.

[18] Wang, P. and Chung, T.S., 2015. Recent advances in membrane distillation processes: Membrane development, configuration design and application exploring. *Journal of membrane science*, *474*, pp.39-56.

[19] Al-Obaidani, S., Curcio, E., Macedonio, F., Di Profio, G., Al-Hinai, H. and Drioli, E., 2008. Potential of membrane distillation in seawater desalination: thermal efficiency, sensitivity study and cost estimation. *Journal of Membrane Science*, *323*(1), pp.85-98.

[20] Imdad, A., Ahmed, I. and Tofique, A., 2018. *Solar Driven Membrane Distillation Unit*, School of Mechanical and Manufacturing Engineering (SMME), National University of Sciences and Technology NUST, pp.69-72.

[21] Martınez-Dıez, L., Vázquez-González, M.I. and Florido-Dıaz, F.J., 1998. Study of membrane distillation using channel spacers. *Journal of membrane science*, *144*(1-2), pp.45-56.

[22] Martinez, L. and Rodríguez-Maroto, J.M., 2006. Characterization of membrane distillation modules and analysis of mass flux enhancement by channel spacers. *Journal of Membrane Science*, *274*(1-2), pp.123-137.

[23] Martinez, L. and Rodríguez-Maroto, J.M., 2007. Effects of membrane and module design improvements on flux in direct contact membrane distillation. *Desalination*, *205*(1-3), pp.97-103.

[24] Martínez-Díez, L. and Vazquez-Gonzalez, M.I., 1999. Temperature and concentration polarization in membrane distillation of aqueous salt solutions. *Journal of membrane science*, *156*(2), pp.265-273.

[25] Subramani, A., Kim, S. and Hoek, E.M., 2006. Pressure, flow, and concentration profiles in open and spacer-filled membrane channels. *Journal of Membrane Science*, *277*(1-2), pp.7-17.

[26] Chang, H., Hsu, J.A., Chang, C.L. and Ho, C.D., 2015. CFD study of heat transfer enhanced membrane distillation using spacer-filled channels. *Energy Procedia*, *75*, pp.3213-3219.

[27] Shirazi, M.M.A., Kargari, A., Ismail, A.F. and Matsuura, T., 2016. Computational fluid dynamic (CFD) opportunities applied to the membrane distillation process: State-of-the-art and perspectives. *Desalination*, *377*, pp.73-90.

[28] Katsandri, A., 2017. A theoretical analysis of a spacer filled flat plate membrane distillation modules using CFD: Part II: Temperature polarisation analysis. *Desalination*, *408*, pp.166-180.

[29] Katsandri, A., 2017. A theoretical analysis of a spacer filled flat plate membrane distillation modules using CFD: Part I: velocity and shear stress analysis. *Desalination*, *408*, pp.145-165.

[30] Chang, H., Hsu, J.A., Chang, C.L., Ho, C.D. and Cheng, T.W., 2017. Simulation study of transfer characteristics for spacer-filled membrane distillation desalination modules. *Applied Energy*, *185*, pp.2045-2057.

[31] Shakaib, M., Hasani, S.M.F., Haque, M.E.U., Ahmed, I. and Yunus, R.M., 2013. A CFD study of heat transfer through spacer channels of membrane distillation modules. *Desalination and Water Treatment*, *51*(16-18), pp.3662-3674.

[32] Al-Sharif, S., Albeirutty, M., Cipollina, A. and Micale, G., 2013. Modelling flow and heat transfer in spacer-filled membrane distillation channels using open source CFD code. *Desalination*, *311*, pp.103-112.

[33] Cipollina, A., Micale, G. and Rizzuti, L., 2011. Membrane distillation heat transfer enhancement by CFD analysis of internal module geometry. *Desalination and Water Treatment*, *25*(1-3), pp.195-209.

[34] Phattaranawik, J., Jiraratananon, R., Fane, A.G. and Halim, C., 2001. Mass flux enhancement using spacer filled channels in direct contact membrane distillation. *Journal of membrane science*, *187*(1-2), pp.193-201.

[35] Phattaranawik, J., Jiraratananon, R. and Fane, A.G., 2003. Effects of net-type spacers on heat and mass transfer in direct contact membrane distillation and comparison with ultrafiltration studies. *Journal of membrane science*, *217*(1-2), pp.193-206.

[36] Song, L. and Ma, S., 2005. Numerical studies of the impact of spacer geometry on concentration polarization in spiral wound membrane modules. *Industrial & engineering chemistry research*, *44*(20), pp.7638-7645.

[37] Ma, S. and Song, L., 2006. Numerical study on permeate flux enhancement by spacers in a crossflow reverse osmosis channel. *Journal of Membrane Science*, *284*(1-2), pp.102-109.

[38] Guillen, G. and Hoek, E.M., 2009. Modeling the impacts of feed spacer geometry on reverse osmosis and nanofiltration processes. *Chemical Engineering Journal*, *149*(1-3), pp.221-231.

[39] Yang, X., Yu, H., Wang, R. and Fane, A.G., 2012. Analysis of the effect of turbulence promoters in hollow fiber membrane distillation modules by computational fluid dynamic (CFD) simulations. *Journal of membrane science*, *415*, pp.758-769.

[40] Shakaib, M., Hasani, S.M.F., Ahmed, I. and Yunus, R.M., 2012. A CFD study on the effect of spacer orientation on temperature polarization in membrane distillation modules. *Desalination*, *284*, pp.332-340.

[41] Cipollina, A., Di Miceli, A., Koschikowski, J., Micale, G. and Rizzuti, L., 2009. CFD simulation of a membrane distillation module channel. *Desalination and Water Treatment*, *6*(1-3), pp.177-183.

[42] Martınez-Dıez, L., Vázquez-González, M.I. and Florido-Dıaz, F.J., 1998. Study of membrane distillation using channel spacers. *Journal of membrane science*, *144*(1-2), pp.45-56.

[43] Martinez, L. and Rodríguez-Maroto, J.M., 2006. Characterization of membrane distillation modules and analysis of mass flux enhancement by channel spacers. *Journal of Membrane Science*, *274*(1-2), pp.123-137.

Chapter 7: Appendix

Material Properties for Feed Channel

Property	Value
Density (kgm^{-3})	998.2
Specific Heat (C_p) ($J\ kg^{-1}\ K^{-1}$)	4182
Thermal Conductivity ($Wm^{-1}K^{-1}$)	0.6
Viscosity ($kg\ m^{-1}\ s^{-1}$)	Piecewise Polynomial function

Material Properties for Permeate Channel

Property	Value
Density (kgm^{-3})	997.5
Specific Heat (C_p) ($J\ kg^{-1}\ K^{-1}$)	4182
Thermal Conductivity ($Wm^{-1}K^{-1}$)	0.65
Viscosity ($kg\ m^{-1}\ s^{-1}$)	Piecewise Polynomial function

Material Properties for Membrane

Property	Value
Density (kgm^{-3})	22000
Specific Heat (C_p) ($J\ kg^{-1}\ K^{-1}$)	1000
Thermal Conductivity ($Wm^{-1}K^{-1}$)	0.2

Viscosity – Temperature Relationship

The relation was developed using Excel by plotting values of Viscosity against temperature for temperature range of 283 K to 373 K.

$$y = 2 \times 10^{-8}x^4 - 3 \times 10^{-5}x^3 + 0.0137x^2 - 3.2283x + 287.54$$

Values of Viscosity in the temperature range is given by the following relation for water.

$$\mu = 2.41 \times 10^{-5} \exp\left(\frac{247.8}{T - 140}\right)$$